https://doi.org/10.5194/acp-2020-150
Preprint. Discussion started: 21 February 2020


Atmospheric Chemistry and Physics Discussions

# The promotion effect of nitrous acid on aerosol formation in wintertime Beijing: possible contribution of traffic-related emission

Yongchun Liu[1*], Yusheng Zhang[1], Chaofan Lian[2,6], Chao Yan[3], Zeming Feng[1], Feixue Zheng[1], Xiaolong Fan[1], Yan Chen[2,6], Weigang Wang[2,6*], Biwu Chu[3,4], Yonghong Wang[3], Jin Cai[3], Wei Du[3], Kaspar R. Daellenbach[3], Juha Kangasluoma[1,3], Federico Bianchi[1,3], Joni Kujansuu[1,3], Tuukka Petäjä[3], Xuefei Wang[6], Bo Hu[5], Yuesi Wang[5], Maofa Ge[2], Hong He[4] and Markku Kulmala[1,3*]

1. Aerosol and Haze Laboratory, Advanced Innovation Center for Soft Matter Science and Engineering, Beijing University of Chemical Technology, Beijing, 100029, China

2. State Key Laboratory for Structural Chemistry of Unstable and Stable Species, Beijing National Laboratory for Molecular Sciences, Institute of Chemistry, Chinese Academy of Sciences, Beijing 100190, China

3. Institute for Atmospheric and Earth System Research/Physics, Faculty of Science, University of Helsinki, P.O. Box 64, FI-00014, Finland

4. State Key Joint Laboratory of Environment Simulation and Pollution Control, Research Center for Eco-Environmental Sciences, Chinese Academy of Sciences, Beijing, 100085, China

5. State Key Laboratory of Atmospheric Boundary Layer Physics and Atmospheric Chemistry, Institute of Atmospheric Physics, Chinese Academy of Sciences, Beijing, 100029, China

6. University of Chinese Academy of Sciences, Beijing 100049, PR China

*Correspondence to:* liuyc@buct.edu.cn, wangwg@iccas.ac.cn or markku.kulmala@helsinki.fi

https://doi.org/10.5194/acp-2020-150
Preprint. Discussion started: 21 February 2020


Atmospheric Chemistry and Physics Discussions


## Abstract

Secondary aerosol is a major component of $PM_{2.5}$, yet its formation mechanism in the ambient atmosphere is still an open question. Based on field measurements in downtown Beijing, we show that the photolysis of nitrous acid (HONO) could promote the formation of organic and nitrate aerosol in wintertime Beijing as evidenced by the growth of the mass concentration of organic and nitrate aerosols linearly increasing as a function of consumed HONO from early morning to noon. The increased nitrate also lead to the formation of particulate matter ammonium by enhancing the neutralization of nitric acid by ammonia. We further illustrate that over 50 % of the ambient HONO during pollution events in wintertime Beijing might be related to traffic-related emission including direct emission and formation via the reaction between OH and vehicle-emitted NO. Overall, our results highlight that the traffic-related HONO plays an important role in the oxidative capacity and in turn, contribute to the haze formation in winter Beijing. Mitigation of HONO and $NO_x$ emission from the vehicles might be an effective way to reduce secondary aerosol mass formation and severe haze events in wintertime Beijing.

https://doi.org/10.5194/acp-2020-150
Preprint. Discussion started: 21 February 2020


Atmospheric Chemistry and Physics Discussions

## 1. Introduction

China is one of the most suffering countries from the pollution of fine particulate matter with diameter less than 2.5 μm ($PM_{2.5}$) (Lelieveld et al., 2015). Although the regional air quality has been continuously improving since the central government of China issued the Clean Air Act in 2013 (Vu et al., 2019), $PM_{2.5}$ concentration is still significantly higher than that in developed countries (Fu et al., 2014;An et al., 2019). Nowadays, a consensus has been reached that haze events are driven by local emissions (An et al., 2019), regional transport (Zheng et al., 2015b) and secondary formation (Huang et al., 2014;He et al., 2018) of pollutants under unfavorable meteorological conditions (stagnant atmosphere and high relative humidity) (Zhu et al., 2018;Liu et al., 2017c). A feedback loop between meteorological parameters and haze formation has also been found playing an important role in the evolution of haze events (Zhang et al., 2018).

Secondary aerosol can contribute up to ~70 % to the aerosol mass concentration in polluted days (Huang et al., 2014). Several reaction pathways have been proposed in the atmospheric chemistry community, such as sulfate formation via heterogeneous oxidation of $SO_2$ promoted by $H_2O_2$ and/or $NO_2$ on mineral dust (Huang et al., 2015;He et al., 2014), aqueous oxidation of $SO_2$ promoted by $NO_2$ in the presence or absence of $NH_3$ in particle-bound water film (He et al., 2014;Wang et al., 2016), catalytic conversion of $SO_2$ to sulfate by black carbon (Zhang et al., 2020), nitrate formation via efficient hydrolysis of $N_2O_5$ on aerosol surfaces (Wang et al., 2017c;Wang et al., 2019;Kulmala, 2018;Li et al., 2017), and the haze formation initiated by new particle

https://doi.org/10.5194/acp-2020-150
Preprint. Discussion started: 21 February 2020


Atmospheric Chemistry and Physics Discussions

formation and growth (Guo et al., 2014;Guo et al., 2020). During the past years, strict control of coal combustion has successfully reduced the $SO_2$ concentration, resulting in a reduction of sulfate ($SO_4^{2-}$) component in $PM_{2.5}$; in stark contrast, the contributions from organic and nitrate become increasingly more significant in China (Lang et al., 2017).

The formation of secondary organic aerosol (SOA) starts from the gas-phase oxidation of volatile organic compounds (VOCs) leading to various oxidized low-volatility and semi-volatile products (Bianchi et al., 2019), followed by their partitioning into the particle phase (Hallquist et al., 2009). Similarly, the formation of nitrate aerosol in the daytime is largely due to the partitioning of gaseous nitric acid, which is formed via the oxidation of $NO_2$ by OH (Seinfeld and Pandis, 2006;Wang et al., 2019). It is traditionally believed that the wintertime atmospheric oxidation capacity is weak due to the weak solar radiation, which limits the formation of SOA and nitrate (Sun et al., 2013). However, it is very recently shown that the peak OH concentration in polluted days in winter Beijing varies from $2\times10^6$ to $6\times10^6$ molecules $cm^{-3}$, which is 6-10 times higher than what is predicted by the global model (Tan et al., 2018). This discrepancy can be largely reduced after accounting for other OH production processes in model simulations, which shows that the photolysis of nitric acid (HONO) dominates the OH production in wintertime Beijing (Tan et al., 2018), and some other cities (Ren et al., 2006;Stutz et al., 2013).

More recently, modelling studies have suggested that nitrous acid (HONO) could enhance secondary aerosols formation in Beijing-Tianjin-Hebei (BTH) region (Zhang

https://doi.org/10.5194/acp-2020-150
Preprint. Discussion started: 21 February 2020


Atmospheric Chemistry and Physics Discussions

et al., 2019b) and Pearl-River-Delta (PRD) region of China (Zhang et al., 2019a;Xing et al., 2019). These results imply that the role of HONO in haze chemistry might be crucial in wintertime Beijing, while the direct evidence from observation has not been reported, yet. On the other hand, the HONO budget has been investigated via modelling studies (Liu et al., 2019c;Zhang et al., 2019b) and photostationary state calculations (Wang et al., 2017b;Li et al., 2018;Huang et al., 2017;Lee et al., 2016;Oswald et al., 2015) at different locations. It is important to analyze the HONO budget in polluted events for understanding the possible influence of HONO sources on secondary pollutants formation.

In this work, we carried out comprehensive measurements at a newly constructed observation station (Aerosol and Haze Laboratory, Beijing University of Chemical Technology, AHL/BUCT Station) located in the western campus of Beijing University of Chemical Technology in downtown Beijing. We show observational evidence that HONO has a prominent promotion effect on the secondary aerosol mass formation in winter. Traffic-related emission seems to be a vital contributor to ambient HONO during the pollution events in winter in Beijing.

## 2. Materials and methods

**2.1 Field measurements.** Field measurements were performed at AHL/BUCT Station (Lat. 39º56′31″ and Lon. 116º17′52″) from February 1 to June 30, 2018. The observation station is on a rooftop of the main building, which is 550 m from the 3rd ring road in the East, 130 m from the Zizhuyuan road in the North and 565 m from the Nandianchang road in the West (Figure S1). The station is surrounded by both traffic

https://doi.org/10.5194/acp-2020-150
Preprint. Discussion started: 21 February 2020


Atmospheric Chemistry and Physics Discussions

and residential emissions, thus, is a typical urban observation site.

Ambient air was sampled from the roof of the main building with five floors (~18 m above the surface). A $PM_{2.5}$ inlet (URG) was used to cut off the particles with diameter larger than 2.5 μm before going to a Nafion dryer (MD-700-24, Perma Pure). Then a Time-of-Flight Aerosol Chemical Speciation Monitor (ToF-ACSM, Aerodyne) and an Aethalometer (AE33, Magee Scientific) were connected to the manifold of aerosol sampling tube. The Reynolds number in the aerosol sampling tube was 800 with the total flow rate of 16.7 lpm and the residence time of 6.5 s. The details about ToF-ACSM measurement was described in the Supplement information. Ambient air was drawn from the roof using a Teflon sampling tube (BMET-S, Beijing Saak-Mar Environmental Instrument Ltd.) with the residence time <10 s for gas phase pollutants measurements. Trace gases including NOx, $SO_2$, CO and $O_3$ were measured with the corresponding analyzer (Thermo Scientific, 42i, 43i, 48i and 49i). Volatile organic compounds (VOCs) was measured using an online Single Photon Ionization Time-of-flight Mass Spectrometer (SPI-ToF-MS 3000R, Hexin Mass Spectrometry) with unit mass resolution (UMR). The principle and the configuration of the instrument has been described in detail elsewhere (Gao et al., 2013) and the Supplement information. HONO concentration was measured using a home-made Long Path Absorption Photometer (LOPAP) (Tong et al., 2016). The details are described in the Supplement information. Particle size and number concentration from 1 nm to 10 μm were measured with Scanning Mobility Particle Sizer (SMPS 3936, TSI), particle size magnifier (PSM, Airmodus) and Neutral Cluster and Air Ion Spectrometer (NIAS, Airel Ltd.).

https://doi.org/10.5194/acp-2020-150
Preprint. Discussion started: 21 February 2020


Atmospheric Chemistry and Physics Discussions

Meteorological parameters including temperature, pressure, relative humidity (RH), wind speed and direction were measured using a weather station (AWS310, Vaisala). Visibility and planetary boundary layer (PBL) height were measured using a visibility sensor (PWD22, Vaisala) and a ceilometer (CL51,Vaisala), respectively

**2.2 HONO budget calculation.** Multiple sources of ambient HONO have been identified, such as emission from soil ($E_{soil}$) (Oswald et al., 2015;Meusel et al., 2018) and vehicle exhaust ($E_{vehicle}$) (Trinh et al., 2017), production through homogeneous reaction between NO and OH ($P_{NO\text{-}OH}$) in the atmosphere, photolysis of nitrate ($P_{nitrate}$) (Bao et al., 2018), nitrous acid ($P_{HNO3}$) and nitrophenenol ($P_{nitrophenol}$) (Sangwan and Zhu, 2018), heterogeneous reaction of $NO_2$ on aerosol surface ($P_{aerosol}$) (Liu et al., 2015) and ground surface ($P_{ground}$) (Liu et al., 2019c;Li et al., 2018;Wang et al., 2017b). However, the photolysis of $HNO_3$ and nitrophenol were excluded in this work because they were believed as minor sources (Lee et al., 2016) and their concentrations were unavailable during our observation. The removal pathways of HONO including photolysis ($L_{photolysis}$), the homogeneous reaction with OH radical ($L_{HONO\text{-}OH}$) and dry deposition ($L_{deposition}$) (Liu et al., 2019c) were considered.

The stationary state HONO concentration could be calculated by (1),

$$\frac{dc_{HONO}}{dt} = E_{HONO} + P_{HONO} - L_{HONO} \quad (1)$$

where $\frac{dc_{HONO}}{dt}$ is the observed change rate of HONO mixing ratios (ppbv $h^{-1}$); $E_{HONO}$ represents the emission rate of HONO from different sources (ppbv $h^{-1}$); $P_{HONO}$ is the in-*situ* production rate of HONO in the troposphere (ppbv $h^{-1}$); $L_{HONO}$ is the loss rate of HONO (ppbv $h^{-1}$) (Li et al., 2018).

https://doi.org/10.5194/acp-2020-150
Preprint. Discussion started: 21 February 2020


Atmospheric Chemistry and Physics Discussions

The emission rate ($E_{HONO}$, ppbv $h^{-1}$) was calculated based on the emission flux ($F_{HONO}$, g $m^{-2}$ $s^{-1}$) and PBL height ($H$, m) according to the following equation,

$$E_{HONO} = \frac{\alpha \cdot F_{HONO}}{H} \quad (2)$$

where, α is the conversion factor ($\alpha = \frac{1\times10^{9}\cdot3600\cdot R\cdot T}{M\cdot P} = \frac{2.99\times10^{13}\cdot T}{M\cdot P}$), $M$ is the molecular weight (g $mol^{-1}$), $T$ is the temperature (K) and $P$ is the atmospheric pressure (Pa).

The production rates of HONO ($P_{HONO}$, ppbv $h^{-1}$) in the troposphere was calculated by,

$$P_{HONO} = 3600 \cdot k_1 \cdot c_{precursor} \quad (3)$$

where, $k_1$ is the quasi first-order reaction rate constant ($s^{-1}$), $c_{precursor}$ is the concentration of precursor (ppbv). For homogeneous reaction between NO and OH,

$$k_1 = k_2 \cdot c_{OH} \quad (4)$$

where, $k_2$ is the second-order reaction rate constant ($7.2\times10^{-12}$ $cm^3$ $molecule^{-1}$ $s^{-1}$) (Li et al., 2012), $c_{OH}$ is the OH concentration (molecules $cm^{-3}$). For heterogeneous reaction,

$$k_1 = \frac{\gamma \cdot A_s \cdot \omega}{4} \cdot Y_{HONO} \quad (5)$$

where, $A_s$ is the surface area concentration of the reactive surface ($m^2$ $m^{-3}$), $\omega$ is the molecular mean speed (m $s^{-1}$), γ is the uptake coefficient of the precursor, $Y_{HONO}$ is the yield of HONO. For ground surface, the surface area concentration is

$$A_s = \frac{\delta}{H} \quad (6)$$

where $\delta$ is the surface roughness, which is calculated according to the mean project area, perimeter and height of the buildings in Beijing.

$$\delta = \frac{f_{building} * (A_{projected} + h * P_{building})}{A_{projected}} * f_{blank} \quad (7)$$

where $f_{building}$ (0.31) and $f_{blank}$ (0.69) are the fraction of the projected area ($A_{projected}$) of

https://doi.org/10.5194/acp-2020-150
Preprint. Discussion started: 21 February 2020


Atmospheric Chemistry and Physics Discussions

buildings and blank space, respectively; $P_{building}$ and $h$ are the perimeter and the height of the building, respectively. $f_{building}$ and $P_{building}$ are measured by ImageJ software based on Google Map. The mean height (44.5 m) of the building in Beijing is linearly extrapolated from the literature data based on remote measurement using Light Detection and Ranging (LiDAR) sensor from 2004 to 2008 (Cheng et al., 2011).

As for photolysis reaction, the first-order reaction rate was

$$k_1 = J \quad (8)$$

where, $J$ is the photolysis rate to produce HONO ($s^{-1}$).

The loss rates of HONO by photolysis ($L_{photolysis}$), homogeneous reaction with OH radicals ($L_{HONO\text{-}OH}$) and dry deposition ($L_{deposition}$) (Liu et al., 2019c) were calculated according to the following equations.

$$L_{photolysis} = 3600 \cdot J_{HONO} \cdot c_{HONO} \quad (9)$$

$$L_{HONO-OH} = 3600 \cdot k_{HONO-OH} \cdot c_{OH} \cdot c_{HONO} \quad (10)$$

$$L_{deposition} = \frac{3600 \cdot v_d \cdot c_{HONO}}{H} \quad (11)$$

where, $J_{HONO}$ is the photolysis rate of HONO ($s^{-1}$), $k_{HONO\text{-}OH}$ is the second-order reaction rate constant between HONO and OH ($6\times10^{-12}$ $cm^3$ $molecule^{-1}$ $s^{-1}$) (Atkinson et al., 2004), and $v_d$ is the dry deposition rate of HONO (0.001 m $s^{-1}$) (Han et al., 2017).

In addition, even though all the current known sources had been considered in models, the modelled daytime HONO concentrations were still lower than the observed concentration (Tang et al., 2015;Michoud et al., 2014). Therefore, the HONO concentration could be described in equation (12).

$$\frac{dc_{HONO}}{dt} = E_{soil} + E_{vehicle} + P_{NO-OH} + P_{nitrate} + P_{aerosol} + P_{ground} + P_{unknown} -$$

https://doi.org/10.5194/acp-2020-150
Preprint. Discussion started: 21 February 2020


Atmospheric Chemistry and Physics Discussions

$$L_{photolysis} - L_{HONO-OH} - L_{deposition} \quad (12)$$

## 3. Results and discussion

**3.1 Overview of the air pollution.** The mass concentration of non-refractory $PM_{2.5}$ (NR-$PM_{2.5}$) and HONO are shown in Fig. 1. The time series of other pollutants ($SO_2$, NOx, CO, $O_3$, benzene, toluene, $PM_{2.5}$ and black carbon) and metrological parameters including wind direction, wind speed, pressure, visibility, RH and temperature are shown in Fig. S2 in the Supplement Materials.

Similar to previous measurements (Guo et al., 2014;Wang et al., 2016), the air pollution events showed a periodic cycle of 3-5 days during the observation, as indicated by the concentration of NR-$PM_{2.5}$ (Fig. 1A), gaseous pollutants and the visibility (Fig. S2). During the observation period, 20-60% of hourly $PM_{2.5}$ concentration was higher than 75 μg $m^{-3}$ in each month (Fig. S3A). In particular, the frequency of severe polluted episodes in March was obviously higher than that in the rest months (Fig. 1 and S3), resulting in the highest monthly mean concentration of $PM_{2.5}$ (88.5±60.0 μg $m^{-3}$) and NR-$PM_{2.5}$ (67.0±56.8 μg $m^{-3}$). This can be explained by both intensive emission during the heating season, which is supported by the high concentration of primary pollutants including CO, $SO_2$ and BC (Table S1), and the stagnant meteorological conditions that physically and chemically promote the accumulation of pollutants. For example, the low wind speed (<2 m $s^{-1}$) mainly from south-based directions accompanied with the low planetary boundary layer (PBL) height frequently occurred in March compared with other months (Fig. S4A).

OA and nitrate dominated the NR-$PM_{2.5}$, while their relative contribution varied

https://doi.org/10.5194/acp-2020-150
Preprint. Discussion started: 21 February 2020


Atmospheric Chemistry and Physics Discussions

significantly during the observation (Fig. 1B and Table S1). This is similar to the previously reported NR-$PM_{1.0}$ composition (Sun et al., 2015). The monthly mean fraction of OA varied from 45.9±10.2 % to 52.6±18.7 %, which was accompanied by a slight increase of sulfate from 16.0±9.1 % to 18.2±8.0 % (Fig. S4D). At the same time, nitrate and chloride decreased from 26.7±8.8 % to 16.7±12.8 % and from 7.7±6.1 % to 0.3±0.2 %, respectively. Ammonium showed a peak value (14.2±2.8 %) in March, then slightly decreased to 12.2±5.2 %. The intensive emission of chloride from coal combustion during heating season (Cho et al., 2008) and firework burning (Zhang et al., 2017), which was transported from Tangshan during Chinese New Year (Fig. S5A and B), led to high fraction of chloride in February and March. The decrease in nitrate and ammonium fractions from February to June should be related to the increasing in temperature (Fig. S2) which was in favor of $NH_4NO_3$ decomposition (Wang et al., 2015). Besides the reduction of the contribution from other components, secondary formation due to increased UV light (Figure S4C) might also favor the increased OA fraction.

It should be noted that the median mass concentrations of nitrate and OA also were higher in March than that in other months (Fig. S4C). The median mass concentrations of nitrate were 1.42, 8.76, 6.30, 3.15, and 3.23 μg $m^{-3}$ from February to June, respectively. And the corresponding OA concentrations were 4.78, 14.04, 11.64, 13.89, and 14.08 μg $m^{-3}$. Secondary formation is the major source of OA and nitrate in the atmosphere (Huang et al., 2014). This means that chemical transformation in March should still be vigorous although the UV light intensity in March is lower than in summer (Fig. S4C). It also implies other factors may compensate the weak UV light

https://doi.org/10.5194/acp-2020-150
Preprint. Discussion started: 21 February 2020


Atmospheric Chemistry and Physics Discussions

intensity in March.

HONO, which has been recognized as the important precursor of OH radical (Ren et al., 2006;Alicke et al., 2003), ranged from 0.05 to 10.32 ppbv from February 1 to June 30, 2018 (Fig. 1C) with the mean value of 1.26±1.06 ppbv. In winter (February and March), HONO concentration was 1.15±1.10 ppbv and comparable to the previous results (1.05±0.89 ppbv) measured in the winter of Beijing (Wang et al., 2017b;Hou et al., 2016), while it was slightly lower than that from April to June (1.35±1.11 ppbv) in this work and those measured in the summer of Shanghai (2.31 ppbv, in May) (Cui et al., 2018) and Guangzhou (2.8 ppbv, in July) (Qin et al., 2009). The mean HONO concentration in March (1.53±1.25 ppbv) was higher than that in February and April (Fig. S3D), while was slightly higher or close to that in May and June. Chamber studies have found that HONO is responsible for the initiation of photosmog reactions (Rohrer et al., 2005). It is reasonable to postulate that HONO probably play an important in the secondary chemistry of particle formation in March.

**3.2 Promotion effect of HONO photolysis on aerosol formation in winter.** Oxidation of precursors by OH radicals is the main mechanism regarding to secondary aerosol formation in the troposphere. After partially ruling out the possible influence of PBL variation by normalizing the concentrations of all pollutants to CO (Cheng et al., 2016), we found all secondary species including sulfate, nitrate and ammonium show obvious daytime peaks from 7:00 am to 6:00 pm (Figure S5C) (Cheng et al., 2016). The similar trends were observed after the concentrations of pollutants were normalized to BC (not shown). This suggests they might connect with photochemistry.

https://doi.org/10.5194/acp-2020-150
Preprint. Discussion started: 21 February 2020


Atmospheric Chemistry and Physics Discussions

Photolysis of $H_2O_2$, HCHO, $O_3$ and HONO, and in $RO_2$ chemistry are known as sources of OH radical in the atmosphere (Alicke et al., 2003;Volkamer et al., 2010;Tan et al., 2018). In this work, the concentration of $H_2O_2$, HCHO and $RO_2$ are unavailable. Thus, their contributions to OH production were not discussed here. However, it has been well recognized that the photolysis of HONO is the dominating source of OH in the dawn and dusk period (Holland et al., 2003), even contributes up to 60% of daytime OH source in winter (Spataro et al., 2013;Rohrer et al., 2005). Therefore, it is meaningful to discuss the contribution of HONO to secondary aerosol formation through OH production. We simply compared the OH production via photolysis of HONO ($P_{OH\text{-}HONO}$) and $O_3$ ($P_{OH\text{-}O3}$) in Fig. 2 when the $PM_{2.5}$ concentration was larger than 50 μg $m^{-3}$ and the RH was less than 90 %. Under these conditions, local chemistry should be more important as 75 % of the wind speed was less than 1.0 m $s^{-1}$ (Fig. S6). In polluted days in winter, the maximal $P_{OH\text{-}HONO}$ and $P_{OH\text{-}O3}$ were 1.73±0.86 × $10^7$ molecules $cm^{-3}$ $s^{-1}$ (2.43±1.21 ppb $h^{-1}$) and 1.03±1.06 × $10^7$ molecules $cm^{-3}$ $s^{-1}$ (1.45±1.49 ppb $h^{-1}$), respectively (Fig. 2A). Owing to the high HONO concentration accumulated throughout the night, the maximal $P_{OH\text{-}HONO}$ in winter was as about 2-6 times of that was observed in the wintertime of Colorado, USA (~0.59 ppb $h^{-1}$) (Kim et al., 2014), New York, USA (~0.40 ppb $h^{-1}$) (Kanaya et al., 2007) and Nanjing, China (0.90±0.27 ppb $h^{-1}$) (Liu et al., 2019b). In the period from April to June, the daily maxima of $P_{OH\text{-}HONO}$ and $P_{OH\text{-}O3}$ were 2.48±1.42 × $10^7$ molecules $cm^{-3}$ $s^{-1}$ (3.48±1.99 ppb $h^{-1}$) and 6.51±4.17 × $10^7$ molecules $cm^{-3}$ $s^{-1}$ (9.15±5.86 ppb $h^{-1}$), respectively.

As shown in Fig. 2A, the daytime $P_{OH\text{-}HONO}$ was always significantly higher than

https://doi.org/10.5194/acp-2020-150
Preprint. Discussion started: 21 February 2020


Atmospheric Chemistry and Physics Discussions

the $P_{OH\text{-}O3}$ in winter. The hourly averaged $P_{OH\text{-}HONO}/P_{OH\text{-}O3}$ ratio varied in the range of 1-25.4 during the daytime, while it varied from 0.3 to 2.8 from April to June. This means that the photolysis of HONO dominates the daytime OH production in polluted days in winter, while photolysis of $O_3$ behaves as a bigger OH source from April to June. This is consistent with the previous findings that HONO photolysis is the dominant OH source in winter of BTH (Xing et al., 2019;Tan et al., 2018), Colorado and New York City (Ren et al., 2006;Kim et al., 2014), while photolysis of $O_3$ and HCHO usually dominated OH production in summer (Alicke et al., 2003).

Oxidation of trace gas pollutants, in particular VOCs, by OH is their main removal pathway in the troposphere (Atkinson and Arey, 2003). The oxidation products with low volatility can contribute to secondary aerosol formation (Kroll and Seinfeld, 2008). Although the high loading of fine particles in polluted days could reduce the surface solar radiation (Li et al., 2017), subsequently, the OH concentration, the noon-time OH radical concentrations observed in polluted wintertime of Beijing were $2.4\times10^6$ $cm^{-3}$ compared with $3.6\times10^6$ $cm^{-3}$ in clean days (Tan et al., 2018). It was around 2 times compared to places such as Tokyo (Kanaya et al., 2007) and New York City (Ren et al., 2006). A very recent work has found that oxidation of VOCs from local traffic emission is still efficient even under pollution conditions (Guo et al., 2020). This implies that oxidation of atmospheric trace gases by OH may still be highly effective even in wintertime, thereby facilitating the vigorous formation of secondary pollutants in Beijing (Tan et al., 2018). This can be partially ascribed to the high HONO concentration in winter Beijing. To confirm this assumption, 12 episodes in winter were

https://doi.org/10.5194/acp-2020-150
Preprint. Discussion started: 21 February 2020


Atmospheric Chemistry and Physics Discussions

chosen (Fig. 1) to uncover the connection between aerosol formation and HONO photolysis. The 1st, 3rd and 5th episodes were clean days and the other 9 episodes were typical haze events with duration above 2 days. The features of these episodes were summarized in Table S2. Fig. 2C shows the CO-normalized daytime profiles of OA and HONO in the 7th and 12th episodes as two examples. In all selected cases, HONO exhibited quick reduction due to the photolysis after sunrise, and simultaneously, OA concentration started to increase. This is similar to the evolution of the concentration of pollutants in a typical smog chamber experiment. We further show the formation of OA ($\Delta C_{OA}/C_{CO}$) as a function of the consumed HONO ($-\Delta C_{HONO}/C_{CO}$) in Fig. 2D. Except for the 4th episode that was highly affected by firework emission during the Spring Festival, $\Delta C_{OA}/C_{CO}$ showed a linear dependence on $-\Delta C_{HONO}/C_{CO}$ in winter, and the correlation coefficient was 0.75. As the meteorological condition was stagnant during these cases as indicated by the low wind speed (< 1.0 m $s^{-1}$, Fig. S5D), it was reasonable to mainly ascribe the increase of OA concentration to local secondary formation initiated by OH radical from HONO photolysis. This kind of correlation could not be seen for the pollution events from April to June because the OH production was no longer dominated by HONO photolysis as indicated by Fig. 2D. It should be noted that oxidation of biogenic alkenes by $O_3$ might also contribute to OA formation. However, anthropogenic VOCs instead of biogenic VOCs dominated the wintertime VOCs in Beijing (Liu et al., 2017a). Therefore, it is reasonable to conclude that the increase of OA concentration in daytime might be mainly resulted from oxidation of VOCs by OH.

Similar to OA, $\Delta C_{nitrate}/C_{CO}$ in winter also showed good linear correlation with -

https://doi.org/10.5194/acp-2020-150
Preprint. Discussion started: 21 February 2020


Atmospheric Chemistry and Physics Discussions

328 $\Delta C_{HONO}/C_{CO}$ (R=0.67, Fig. S5E), suggesting that the increase of particle-phase nitrate
329 in the daytime should also be promoted by OH radical from HONO photolysis.
330 Interestingly, and $\Delta C_{ammonium}/CO$ also showed a good correlation with $-\Delta C_{HONO}/C_{CO}$
331 (R=0.61, Fig. S5E), although particle-phase ammonium should not be directly related
332 to oxidation of $NH_3$ by OH. We explained the increased ammonium as the result of
333 enhanced neutralization of $HNO_3$ by $NH_3$ (Wang et al., 2018). This was consistent with
334 the recent work which observed the important role of photochemical reactions in
335 daytime nitrate formation, while hydrolysis of $N_2O_5$ mainly contributed to nighttime
336 nitrate (Tian et al., 2019). Although a recent work has found that daytime hydrolysis of
337 $N_2O_5$ on hygroscopic aerosols is also an important source of daytime nitrate in winter
338 Beijing (Wang et al., 2017a), the linearly correlation between $\Delta C_{nitrate}/C_{CO}$ and
339 $\Delta C_{HONO}/C_{CO}$ at least implies that the promotion effect of HONO on nitrate formation
340 could not be excluded. On the other hand, the correlation between $\Delta C_{sulfate}/C_{CO}$ and -
341 $\Delta C_{HONO}/C_{CO}$ was much weaker (R=0.26), suggesting a weak connection between
342 particle-phase sulfate and gas-phase $H_2SO_4$. This was also consistent with the previous
343 understanding that heterogeneous reactions of $SO_2$ were the dominating pathway for
344 sulfate formation (Zheng et al., 2015a;He et al., 2018;Zhang et al., 2020). Overall, this
345 work well supported the recent modeling results that HONO could obviously promote
346 the aerosol production in winter (Zhang et al., 2019a;Zhang et al., 2019b;Xing et al.,
347 2019;An et al., 2013) from the point of view of observation.

348 **3.3 HONO budget in polluted events.** To understand the possible sources of HONO
349 in polluted events in winter, the HONO budget was calculated for the events when the

https://doi.org/10.5194/acp-2020-150
Preprint. Discussion started: 21 February 2020


Atmospheric Chemistry and Physics Discussions

350 $PM_{2.5}$ concentration was larger than 50 μg $m^{-3}$ and the RH was less than 90 % according
351 to the method described in Section 2.2.
352 **Vehicle emission.** The $E_{vehicle}$ was calculated using the relative emission rate of HONO
353 to $NO_x$ and the emission inventory of $NO_x$ from vehicles. Firstly, the ratio of
354 HONO/$NO_x$ was calculated according to the method reported by Xu et al. (Xu et al.,
355 2015) and Li et al. (Li et al., 2018) from the fresh nighttime plumes which were strictly
356 satisfy the following criteria: 1) $NO_x$ > 45 ppb (highest 25% of $NO_x$ data); 2)
357 $\Delta NO/\Delta NO_x > 0.8$, with good correlation between NO and $NO_x$ ($R > 0.9$, $P < 0.05$); 3)
358 Good correlation between HONO and $NO_x$ ($R^2$>0.65, $P < 0.05$); and 4) Dataset from
359 5:00 am to 8:00 am. The mean emission ratio of HONO to $NO_x$ was 1.8±0.5% based
360 on 5 fresh vehicle exhaust plumes during our observation (Table S3). This value is
361 higher than that in Hongkong (1.2±0.4%) (Xu et al., 2015) and Jinan (0.53±0.20%) (Li
362 et al., 2018) using the same method, while is comparable with the result measured in
363 tunnel experiments (2.1%) carried out in Beijing (Yang et al., 2014). Secondly, low
364 HONO concentration should be companied with high $NO_x$ and high ratio of $\Delta NO/\Delta NO_x$
365 if direct emission from vehicles was the major source of HONO and the source from
366 secondary formation was negligible in the urban atmosphere. Therefore, we further
367 estimated the HONO/$NO_x$ ratio using a low limit correlation method (Li et al., 2012).
368 In the 2D space of HONO verse $NO_x$ (Fig. S7), the lowest marge with $\Delta NO/\Delta NOx$
369 larger than 0.8 were chosen for linear correlation. The ratio of $\Delta HONO/\Delta NOx$ is
370 1.17±0.05%. This value is lower than that estimated above, while is very close to that
371 measured in Hongkong (1.2±0.4%) (Xu et al., 2015) and Guangzhou (1.0%) (Li et al.,

https://doi.org/10.5194/acp-2020-150
Preprint. Discussion started: 21 February 2020


Atmospheric Chemistry and Physics Discussions

372 2012). Finally, several studies have measured the direct emission of HONO from
373 vehicle exhaust. The HONO/$NO_x$ was 0.18% from gasoline cars through chassis
374 dynamometer tests in China (Liu et al., 2017d), while it was 0-0.95% for gasoline
375 vehicles and 0.16-1.0 % for diesel vehicles measured under real-world driving test
376 cycles in Japan (Trinh et al., 2017). Thus, three levels of vehicle emission factor were
377 considered. 1.17±0.05% was taken as the middle value, while 0.18% (Liu et al., 2017d)
378 and 1.8 % were the lower limit and the upper limit, respectively.

379 The hourly NOx emission inventory from vehicles in Beijing, with an annual
380 emission rate of 109.9 Gg $yr^{-1}$ (Yang et al., 2019), was used when calculating the $E_{vehicle}$
381 in this work. The calculated middle value of $E_{vehicle}$ was from 0.085±0.038 to 0.34±0.15
382 ppbv $h^{-1}$, which was slightly higher than the daytime emission rate of HONO in Xi'an
383 (Huang et al., 2017). This is reasonable when the vehicle population in Beijing is taken
384 into consideration. The lower limit of $E_{vehicle}$ was 0.013-0.053 ppbv $h^{-1}$, which was close
385 to the estimated emission rate of HONO in Jinan (Li et al., 2018). The upper limit was
386 in the range of 0.13-0.53 ppbv $h^{-1}$.

387 **Soil emission.** The emission flux of HONO from soil depends on the water content, the
388 nitrogen nutrient content and the temperature of soil (Oswald et al., 2013). In this work,
389 we used the emission flux from grassland, which was more representative in Beijing.
390 The influence of water content and temperature on HONO emission has been
391 considered using the parameters reported in the literature (Oswald et al., 2013). Three
392 levels of water content including 25-35%, 35-45% and 45-55% were considered. The
393 temperature dependence of $F_{HONO}$ was calculated using the mean value of the $F_{HONO}$

https://doi.org/10.5194/acp-2020-150
Preprint. Discussion started: 21 February 2020


Atmospheric Chemistry and Physics Discussions

with different water content, while the low limit and upper limit of $F_{HONO}$ were calculated using based on the emission flux from 45-55% of water content and 25-35% of water content, respectively. The lower limit, the middle value and the upper limit of The $E_{soil}$ are 0.0032-0.013, 0.0046±0.0039-0.020±0.20 and 0.0057-0.025 ppbv $h^{-1}$, respectively.

**Homogeneous reaction between NO and OH.** Direct measurement of OH concentration was unavailable in this work, while several methods were used to estimate the ambient OH concentration. In winter in Beijing, it has been found that the OH concentration is linearly correlated with $J_{O1D}$, that's, $c_{OH}=J_{O1D}\times2\times10^{11}$ molecules $cm^{-3}$ (Tan et al., 2019). However, Tan et al (Tan et al., 2018) reported a larger conversion factor ($4.33\times10^{11}$ molecules $cm^{-3}$). Xu et al. (Xu et al., 2015) estimated the OH radical concentration considering both photolysis rate and $NO_2$ concentration, namely,

$$c_{OH}=\frac{4.1\times10^{9}\times(J_{O1D})^{0.83}\times(J_{NO_2})^{0.19}\times(140c_{NO_2}+1)}{0.41c_{NO_2}^{2}+1.7c_{NO_2}+1} \quad (13)$$

Overall, the estimated OH concentrations according to equation (13) were comparable with that estimated by Tan et al. (Tan et al., 2019) (Fig. S8D). In polluted days, high concentration of $NO_2$ resulted into lower OH concentrations estimated using the equation (13). Therefore, the corresponding $P_{NO\text{-}OH}$ was taken as the low limit for homogeneous reaction between NO and HONO because polluted events were discussed in this work, while $P_{NO\text{-}OH}$ calculated using the OH concentration ($J_{O1D}\times4.33\times10^{11}$ molecules $cm^{-3}$) (Tan et al., 2018) was taken as the upper limit. In the night, OH concentration usually varied from $1.0\times10^{5}$ molecules $cm^{-3}$ (Li et al., 2012;Tan et al., 2018) in winter to $5\times10^{5}$ molecules $cm^{-3}$ in summer (Tan et al., 2017). In this work, the

https://doi.org/10.5194/acp-2020-150
Preprint. Discussion started: 21 February 2020


Atmospheric Chemistry and Physics Discussions

nighttime OH concentration was estimated linearly correlated with the nighttime temperature. Thus, the lower limit, the middle value and the upper limit of $P_{NO\text{-}OH}$ were 0.011-0.039, 0.029±0.053-0.098±0.78 and 0.058-1.96 ppbv $h^{-1}$, respectively. The calculated middle value of $P_{NO\text{-}OH}$ was comparable with those estimated by Li et al. (Li et al., 2018) and Huang et al. (Huang et al., 2017). It should be noted that measured NO concentration was used to calculate the $P_{NO\text{-}OH}$. Besides vehicle emission, power plant and industries also contribute NO emission. 40 % of NOx was from vehicle emission according to the emission inventory of $NO_x$ in Beijing (He et al., 2002). Therefore, the lower limit, the middle value and the upper limit of $P_{NO\text{-}OH}$ from traffic source were 0.0044-0.015, 0.012±0.021-0.39±0.32 and 0.023-0.79 ppbv $h^{-1}$, respectively.

**Photolysis of nitrate.** A recent work reported the photolysis rate of nitrate ($J_{nitrate}$) in ambient $PM_{2.5}$ (Bao et al., 2018). The $J_{nitrate}$ varied from $1.22\times10^{-5}$ to $4.84\times10^{-4}$ $s^{-1}$ with the mean value of $8.24\times10^{-5}$ $s^{-1}$ after normalized to the tropical noontime conditions on the ground. These values were used to calculate the low limit, upper limit and the mean $J_{nitrate}$. The $J_{nitrate}$ during our observation in Beijing was corrected in the light of the latitude and the real sunlight intensity at our station. The corresponding daytime lower limit, the middle value and the upper limit of HONO from photolysis of nitrate were 0.0011-0.096, 0.0072±0.0021-0.66±0.092 and 0.042-3.86 ppbv $h^{-1}$, respectively.

**Heterogeneous reactions of $NO_2$ on aerosol and ground surface.** The production of HONO from heterogeneous reactions of $NO_2$ on aerosol surface was calculated according to equations (3) and (5). The aerosol surface concentration was measured with a SMPS. The uptake coefficient ($\gamma$) of $NO_2$ on different particles varied from $5\times10^{-}$

https://doi.org/10.5194/acp-2020-150
Preprint. Discussion started: 21 February 2020


Atmospheric Chemistry and Physics Discussions

$^{9}$ to $9.6\times10^{-6}$ (Ndour et al., 2009;Underwood et al., 2001;Underwood et al., 1999), while it was recommended to be $1.2\times10^{-8}$ (Crowley et al., 2010). It has been found that the γ highly depends on the relative humidity (RH). The low limit bound of $P_{aerosol}$ was calculated based on the RH dependent uptake coefficient of $NO_2$ on kaolinite, while the upper limit of $P_{aerosol}$ was calculated according to the RH dependent γ on hematite (Liu et al., 2015). Heterogeneous reaction of $NO_2$ on black carbon (BC) was also considered. The surface area concentration of BC was calculated according to its specific area (87 $m^2$ $g^{-1}$) (Su et al., 2018) and the measured mass concentration. The $\gamma_{NO2}$ on BC is $1.17\times10^{-5}$, with a HONO yield of 80% (Han et al., 2013). The light enhanced uptake γ of $NO_2$ ($1.9\times10^{-6}$) on mineral dust was further parameterized (Ndour et al., 2008) after normalized to the solar radiation intensity in Beijing.

The contribution of heterogeneous reaction of $NO_2$ on ground surface was calculated similar to that on mineral dust. The same kinetics for heterogeneous reaction of $NO_2$ on aerosol surface were used to calculate the nighttime contribution of ground surface. A recent work observed a significant enhancement of $NO_2$ and HONO formation by UV light on the real urban grime (Liu et al., 2019a). Thus, RH dependent kinetic data measured on urban grime was used to calculate the daytime upper limit for heterogeneous uptake of $NO_2$ on the ground surface.

The lower limit, the middle value and the upper limit of $P_{aerosol}$ were 0.00012-0.00025, 0.00043±0.00031-0.0028±0.0023 and 0.0022-0.0050 ppbv $h^{-1}$, respectively. The corresponding values were 0.00027-0.00199, 0.0014±0.00095-0.0089±0.006 and 0.0025-0.060 ppbv $h^{-1}$ for $P_{ground}$. The $P_{aerosol}$ calculated in this work was much lower

https://doi.org/10.5194/acp-2020-150
Preprint. Discussion started: 21 February 2020


Atmospheric Chemistry and Physics Discussions

than that estimated by Huang et al. (Huang et al., 2017) because different calculation methods have been used. In their work, the production rate of HONO was estimated based on the conversion rate (Huang et al., 2017), whilst it was calculated based on the measured aerosol surface area concentration and uptake coefficient of $NO_2$ on different particles in this work. In addition, the calculated $P_{aerosol}$ was 2-4 orders of magnitude lower than other sources due to the very small $\gamma_{NO2}$ on particle surface. It should be pointed out that the initial uptake coefficient ($\gamma_{ini}$) was parameterized in this work. This will overestimate the contribution of heterogeneous reaction of $NO_2$ to HONO source because the steady-state uptake coefficient is usually one order of magnitude lower than $\gamma_{ini}$ (Han et al., 2013;Liu et al., 2015). These results mean that heterogeneous reaction should be unimportant for HONO source.

**Comparison among different HONO sources.** Fig. 3 summarizes the diurnal patterns of each sources with different parameterizations during the pollution events from February to March. The black dots and lines mean the middle values, while the shadow indicates the corresponding lower bound and upper bound. In the nighttime, vehicle and soil emission, and homogeneous reaction between NO and OH were the important sources of HONO. In the daytime, however, photolysis of nitrate and homogeneous reaction between NO and OH dominated the sources of HONO. Heterogeneous reactions of $NO_2$ on aerosol surface and ground surfaces were unimportant compared with other sources because of the very low uptake coefficient.

Fig. 4A-F shows the HONO budget estimated using the middle values among these parameters during the polluted events. Although HONO concentration showed a net

https://doi.org/10.5194/acp-2020-150
Preprint. Discussion started: 21 February 2020


Atmospheric Chemistry and Physics Discussions

decrease during the day, the production rate of HONO was more intense than during the night, but was outcompeted by the photolysis loss. The mean production rate of HONO varied from 0.21 to 1.75 ppbv $h^{-1}$, while the corresponding loss rate was from 0.02 to 2.34 ppbv $h^{-1}$ during the polluted events in winter. The main loss of HONO was the photolysis during the daytime (1.71± 0.44 ppbv $h^{-1}$), whereas it was dry deposition in the nighttime (0.062±0.018 ppbv $h^{-1}$). Direct emission from vehicles exhaust was the largest nighttime source of HONO (0.23±0.06 ppbv $h^{-1}$), followed by homogeneous reaction between NO and OH (0.07±0.02 ppbv $h^{-1}$), emission from soil (0.014±0.005 ppbv $h^{-1}$), heterogeneous reactions of $NO_2$ on the ground surface (0.006±0.002 ppbv $h^{-1}$) and heterogeneous reactions of $NO_2$ on aerosol surface (0.0005±0.0001 ppbv $h^{-1}$). The net production led to the accumulation of nighttime HONO and the maximal HONO concentration (2.67±1.38 ppbv) in the early morning. $P_{NO\text{-}OH}$ and $P_{nitrate}$ dominated the daytime HONO production, with daytime mean values of 0.49±0.35 ppbv $h^{-1}$ and 0.34±0.23 ppbv $h^{-1}$, respectively. As shown in Fig. 4, these six sources still underestimated the daytime sources of HONO. The $P_{unknown}$ was 0.57±0.15 ppbv $h^{-1}$ in February and March, while it was 0.77±0.27 ppbv $h^{-1}$ from April to June.

The $E_{vehicle}$ contributed 70.3±5.4% and 65.3±15.2% to the nighttime HONO sources from February to March and the rest months, respectively, even when the $P_{unknown}$ was taken into consideration. The relative contribution of daytime $E_{vehicle}$ decreased to 16.3±19.2% in winter and 9.9±8.5% from April to June. Thus, the daily mean fraction of the $E_{vehicle}$ was 47.8±29.4% and 42.2±30.0% from February to March and from April to June, respectively. This means that the $E_{vehicle}$ dominates the nighttime

https://doi.org/10.5194/acp-2020-150
Preprint. Discussion started: 21 February 2020


Atmospheric Chemistry and Physics Discussions

HONO source during the polluted events in Beijing, which is consistent with the previous result that vehicle emission was the major nighttime HONO source in BTH (Zhang et al., 2019b). As pointed out in Section 3.3, $E_{vechicle}$ was calculated based on the $NO_x$ inventory from vehicle sector. On the other hand, NO is prone to be quickly converted to $NO_2$ and $NO_z$ (including HONO, $HNO_3$, $N_2O_5$, PAN and organonitrate etc) by $O_3$, $HO_2$, $RO_2$ and OH in the atmosphere. It is reasonable to assume that local traffic emission dominates the ambient NO source in the urban environment. Thus, homogeneous reaction between NO and OH in the atmosphere could also be related to vehicle exhaust. Traffic-related HONO sources ($E_{vehicles}$ +$P_{NO\text{-}OH}$) might contribute 73.0±26.0 % to the wintertime HONO source and 58.6±22.0 % to the HONO source from April to June. Even if 40 % of $NO_x$ was from vehicle exhaust in Beijing (He et al., 2002), traffic-related source ($E_{vehicles}$ + 0.4$P_{NO\text{-}OH}$) might still contribute 57.9±27.8 % to the wintertime HONO source and 48.8±28.8 % of the HONO source from April to June. The contribution of traffic-related source was still an important daytime source of HONO (44.2±14.7 % for $E_{vehicles}$ +$P_{NO\text{-}OH}$, and 27.4±16.7 % for $E_{vehicles}$ + 0.4$P_{NO\text{-}OH}$) in polluted days in winter.

As shown in Fig. 3, uncertainties existed when calculating each HONO source. To further understand the role of traffic emission, we also estimated the lower limit of the traffic-related contribution as follows: 1) the lower limit of $E_{vehicle}$ was obtained by using the lowest reported emission ratio of HONO/$NO_x$ from vehicles (0.18%) (Liu et al., 2017d) rather than 1.17%, which was the empirical value calculated based on the field measurement in Fig. S7; 2) the lower limit for homogeneous reaction between NO

https://doi.org/10.5194/acp-2020-150
Preprint. Discussion started: 21 February 2020


Atmospheric Chemistry and Physics Discussions

and OH radical was calculated according to the method by Xu et al. (Li et al., 2018); 3) the upper limit of the emission rate from soil was estimated using the emission flux of HONO with low water content (Oswald et al., 2013); 4) the upper limit of HONO production rate from heterogeneous reaction of $NO_2$ on the aerosol was calculated using the large RH-dependent uptake coefficient of $NO_2$ on hematite (Liu et al., 2015) rather the value recommended by Crowley et al. (Crowley et al., 2010); 5) the upper limit for heterogeneous reaction on ground surface was calculated using the RH-dependent kinetic data measured on urban grime (Liu et al., 2019a). As shown in Fig. 5, traffic-related source ($E_{vehicles}$ + $P_{NO\text{-}OH}$) contributed 43.3±26.1 % to the wintertime HONO if all NO was assumed to be dominated by local traffic emission, while it was 25.3±15.7 % when 40 % of NO was considered as local traffic emission (He et al., 2002). Under this circumstance, the $P_{unknown}$ of HONO in winter increased to 1.06±0.36 ppbv $h^{-1}$, which was corresponding to 63.2±10.1 % of the HONO source. This means these assumptions might underestimate the contribution of the HONO sources. In addition, $P_{ground}$, $P_{aerosol}$ and $P_{nitrate}$ could be also partially related to traffic emission of $NO_x$ (Lee et al., 2016;Tan et al., 2017). These results mean that the contribution of traffic-related emission should be larger than our estimation in this work. Therefore, our work at least suggests that traffic related emission should be a very important HONO source in winter Beijing although more work is required based on comprehensive modelling studies.

## 4. Conclusions and atmospheric implications.

In this work, the promotion effect of HONO on aerosol mass formation in polluted events was observed based on the good correlation between the growth of OA and

https://doi.org/10.5194/acp-2020-150
Preprint. Discussion started: 21 February 2020


Atmospheric Chemistry and Physics Discussions

548 nitrate mass concentration and the consumed HONO from early morning to noon during
549 the polluted days in winter. This promotion effect could be related to OH production
550 from photolysis of HONO on aerosol formation followed by oxidation process of the
551 corresponding precursors. Our observation supports well the recent modelling studies
552 that HONO may significantly promote secondary aerosol mass formation (Zhang et al.,
553 2019a;Zhang et al., 2019b;Xing et al., 2019;An et al., 2013). Based on stationary state
554 calculations, traffic-related sources (direction emission and conversion of NO from
555 vehicle emission) was found to be an important contributor to HONO source during
556 polluted days in winter in Beijing. This means that HONO from the traffic-related
557 sources can have an important role in aerosol mass formation in the atmosphere.

558 Vehicle population in China is increasing very quickly (Liu et al., 2017b;Wang et
559 al., 2011). Thus, the negative influences of the vehicle emission on air quality will
560 increase especially in populous metropolitan areas (Yang et al., 2019;Guo et al., 2020),
561 such as Beijing and Shanghai, if targeted pollution control technologies are not applied.
562 It has been estimated that the vehicles emission accounted for over 40% of total urban
563 $NO_x$ emissions in Beijing (He et al., 2002). In the atmosphere, $NO_x$ involves very
564 complicated reaction network, from which finally leads to aerosol mass formation and
565 production of ozone in VOC limited environment. At the same time, reactions of $NO_x$
566 also leads to some reactive $NO_z$ species (Seinfeld and Pandis, 2006). In particular,
567 HONO is an important precursor of OH, which governs the conversion of primary
568 pollutants to secondary pollutants in the atmosphere. Besides indirect producing of
569 HONO from NO, the vehicles also directly emits HONO as discussed in this work.

https://doi.org/10.5194/acp-2020-150
Preprint. Discussion started: 21 February 2020


Atmospheric Chemistry and Physics Discussions

570 Even if the low limit of emission factor was used to calculating the HONO source from
571 the vehicles, the traffic-related emission can still be an important source of HONO in
572 winter Beijing. Therefore, this work implies that mitigation of HONO and $NO_x$
573 emission from vehicles might be an effective way to reduce secondary aerosol mass
574 formation and can have a positive effect on severe haze events in wintertime Beijing.

575 It should be pointed out that we only considered $O_3$ and HONO when discussing
576 the sources of OH. Other sources such as $HO_2$ (and $RO_2$) with NO, ozonolysis of
577 alkenes and photolysis of OVOCs might also contribute to OH radicals in the
578 atmosphere (Tan et al., 2018). In the future it will be vital to comprehensively analyze
579 OH sources and to quantify the role of HONO in secondary aerosol mass formation
580 although photolysis of HONO is the major OH source in winter. On the other hand, as
581 discussed in Section 3.3, uncertainties about the HONO budget might originate from
582 the emission factors, OH concentration, and reaction kinetics and so on. To take the
583 next step, it is required to measure the emission factors from vehicle exhaust under real
584 road conditions in the future. When calculating the OH concentration, the factor
585 between OH concentration and $J_{O1D}$ might vary over locations and seasons due to
586 different $NO_x$/VOCs ratio (Holland et al., 2003). Direct measurements of OH
587 concentration would be helpful for decreasing the uncertainty of both OH sources and
588 HONO budget analysis. Finally, it is necessary to quantify the contribution of traffic-
589 related source of HONO on secondary aerosol formation based on modelling studies in
590 the future.

591

https://doi.org/10.5194/acp-2020-150
Preprint. Discussion started: 21 February 2020


Atmospheric Chemistry and Physics Discussions

592 *Data availability*. The experimental data are available upon request to the
593 corresponding authors.

594

595 *Supplement*. The supplement related to this article is available online at:

596

## 597 Author information

598 *Author contributions*. YL, WW and MK designed the experiments. YL wrote the paper
599 and performed HONO budget analysis. YZ, CL, WW, YC, MG and XW carried out
600 HONO measurement. ZF, FZ, JC, WD and KD did aerosol composition measurements.
601 BC and JK did particle size measurements. YW, BH and YW analyzed meteorological
602 data analysis. CY, FB, JK, TP, HH, MG and MK revised the manuscript.

603

## 604 Acknowledgements:

605 This research was financially supported by the National Natural Science Foundation of
606 China (41877306), the Ministry of Science and Technology of the People's Republic of
607 China (2019YFC0214701), Academy of Finland via Center of Excellence in
608 Atmospheric Sciences (272041, 316114, and 315203) and European Research Council
609 vShandong Universityia ATM-GTP 266 (742206), the Strategic Priority Research
610 Program of Chinese Academy of Sciences and Beijing University of Chemical
611 Technology.

612

613

https://doi.org/10.5194/acp-2020-150
Preprint. Discussion started: 21 February 2020


Atmospheric Chemistry and Physics Discussions

## References:

Alicke, B., Geyer, A., Hofzumahaus, A., Holland, F., Konrad, S., Patz, H. W., Schafer, J., Stutz, J., Volz-Thomas, A., and Platt, U.: OH formation by HONO photolysis during the BERLIOZ experiment, J. Geophys. Res.-Atmos., 108, 17, 10.1029/2001jd000579, 2003.

An, J., Li, Y., Chen, Y., Li, J., Qu, Y., and Tang, Y.: Enhancements of major aerosol components due to additional HONO sources in the North China Plain and implications for visibility and haze, Adv. Atmos. Sci., 30, 57-66, 10.1007/s00376-012-2016-9, 2013.

An, Z., Huang, R.-J., Zhang, R., Tie, X., Li, G., Cao, J., Zhou, W., Shi, Z., Han, Y., Gu, Z., and Ji, Y.: Severe haze in northern China: A synergy of anthropogenic emissions and atmospheric processes, Proc. Natl. Acad. Sci. USA, 116, 8657-8666, 10.1073/pnas.1900125116, 2019.

Atkinson, R., and Arey, J.: Atmospheric Degradation of Volatile Organic Compounds, Chem. Rev., 103, 4605-4638, doi: 10.1021/cr0206420, 2003.

Atkinson, R., Baulch, D. L., Cox, R. A., Crowley, J. N., Hampson, R. F., Hynes, R. G., Jenkin, M. E., Rossi, M. J., and Troe, J.: Evaluated kinetic and photochemical data for atmospheric chemistry: Volume I - gas phase reactions of Ox, HOx, NOx and SOx species, Atmos. Chem. Phys., 4, 1461-1738, 10.5194/acp-4-1461-2004, 2004.

Bao, F., Li, M., Zhang, Y., Chen, C., and Zhao, J.: Photochemical Aging of Beijing Urban PM2.5: HONO Production, Environ. Sci. Technol., 52, 6309-6316, 10.1021/acs.est.8b00538, 2018.

Bianchi, F., Kurtén, T., Riva, M., Mohr, C., Rissanen, M. P., Roldin, P., Berndt, T., Crounse, J. D., Wennberg, P. O., Mentel, T. F., Wildt, J., Junninen, H., Jokinen, T., Kulmala, M., Worsnop, D. R., Thornton, J. A., Donahue, N., Kjaergaard, H. G., and Ehn, M.: Highly Oxygenated Organic Molecules (HOM) from Gas-Phase Autoxidation Involving Peroxy Radicals: A Key Contributor to Atmospheric Aerosol, Chem. Rev., 119, 3472-3509, 10.1021/acs.chemrev.8b00395, 2019.

Cheng, F., Wang, C., Wang, J., Tang, F., and Xi, X.: Trend analysis of building height and total floor space in Beijing, China using ICESat/GLAS data, Int. J. Remote Sens., 32, 8823-8835, 2011.

Cheng, Y., Zheng, G., Wei, C., Mu, Q., Zheng, B., Wang, Z., Gao, M., Zhang, Q., He, K., Carmichael, G., Poschl, U., and Su, H.: Reactive nitrogen chemistry in aerosol water as a source of sulfate during haze events in China, Sci. Adv., 2, 10.1126/sciadv.1601530, 2016.

Cho, M.-H., Niles, A., uili Huang, Inglese, J., Austin, C. P., Riss, T., and Xia, M.: A bioluminescent cytotoxicity assay for assessment of membrane integrity using a proteolytic biomarker, Toxicol. In Vitro., 22, 1099-1106, 2008.

Crowley, J. N., Ammann, M., Cox, R. A., Hynes, R. G., Jenkin, M. E., Mellouki, A., Rossi, M. J., Troe, J., and Wallington, T. J.: Evaluated kinetic and photochemical data for atmospheric chemistry: Volume V – heterogeneous reactions on solid substrates, Atmos. Chem. Phys., 10, 9059-9223, doi: 10.5194/acp-10-9059-2010, 2010.

Cui, L., Li, R., Zhang, Y., Meng, Y., Fu, H., and Chen, J.: An observational study of nitrous acid (HONO) in Shanghai, China: The aerosol impact on HONO formation during the haze episodes, Sci. Total Environ., 630, 1057-1070, 10.1016/j.scitotenv.2018.02.063, 2018.

Fu, G. Q., Xu, W. Y., Yang, R. F., Li, J. B., and Zhao, C. S.: The distribution and trends of fog and haze in the North China Plain over the past 30 years, Atmos. Chem. Phys., 14, 11949-11958, 10.5194/acp-14-11949-2014, 2014.

Gao, W., Tan, G., Hong, Y., Li, M., Nian, H., Guo, C., Huang, Z., Fu, Z., Dong, J., Xu, X., Cheng, P., and Zhou, Z.: Development of portable single photon ionization time-of-flight mass spectrometer combined

https://doi.org/10.5194/acp-2020-150
Preprint. Discussion started: 21 February 2020




with membrane inlet, Int. J. Mass Spectrom., 334, 8-12, https://doi.org/10.1016/j.ijms.2012.09.003, 2013.
Guo, S., Hu, M., Zamora, M. L., Peng, J., Shang, D., Zheng, J., Du, Z., Wu, Z., Shao, M., Zeng, L., Molina, M. J., and Zhang, R.: Elucidating severe urban haze formation in China, Proc. Natl. Acad. Sci. USA, 111, 17373-17378, 10.1073/pnas.1419604111, 2014.
Guo, S., Hu, M., Peng, J., Wu, Z., Zamora, M. L., Shang, D., Du, Z., Zheng, J., Fang, X., Tang, R., Wu, Y., Zeng, L., Shuai, S., Zhang, W., Wang, Y., Ji, Y., Li, Y., Zhang, A. L., Wang, W., Zhang, F., Zhao, J., Gong, X., Wang, C., Molina, M. J., and Zhang, R.: Remarkable nucleation and growth of ultrafine particles from vehicular exhaust, Proc. Natl. Acad. Sci. USA, 201916366, 10.1073/pnas.1916366117, 2020.
Hallquist, M., Wenger, J. C., Baltensperger, U., Rudich, Y., Simpson, D., Claeys, M., Dommen, J., Donahue, N. M., George, C., Goldstein, A. H., Hamilton, J. F., Herrmann, H., Hoffmann, T., Iinuma, Y., Jang, M., Jenkin, M. E., Jimenez, J. L., Kiendler-Scharr, A., Maenhaut, W., McFiggans, G., Mentel, T. F., Monod, A., Pr év ôt, A. S. H., Seinfeld, J. H., Surratt, J. D., Szmigielski, R., and Wildt, J.: The formation, properties and impact of secondary organic aerosol: current and emerging issues, Atmos. Chem. Phys., 9, 5155-5236, 10.5194/acp-9-5155-2009, 2009.
Han, C., Liu, Y., and He, H.: Role of Organic Carbon in Heterogeneous Reaction of NO2 with Soot, Environ. Sci. Technol., 47, 3174-3181, 10.1021/es304468n, 2013.
Han, X., Zhang, M. G., Skorokhod, A., and Kou, X. X.: Modeling dry deposition of reactive nitrogen in China with RAMS-CMAQ, Atmos. Environ., 166, 47-61, 10.1016/j.atmosenv.2017.07.015, 2017.
He, H., Wang, Y., Ma, Q., Ma, J., Chu, B., Ji, D., Tang, G., Liu, C., Zhang, H., and Hao, J.: Mineral dust and NOx promote the conversion of SO2 to sulfate in heavy pollution days, Sci. Rep., 4, 10.1038/srep04172, 2014.
He, K., Huo, H., and Zhang, Q.: Urban air pollution in China: current status, characteristics, and progress, Annu. Rev. Energ. Env., 27, 397-431, 2002.
He, P. Z., Alexander, B., Geng, L., Chi, X. Y., Fan, S. D., Zhan, H. C., Kang, H., Zheng, G. J., Cheng, Y. F., Su, H., Liu, C., and Xie, Z. Q.: Isotopic constraints on heterogeneous sulfate production in Beijing haze, Atmos. Chem. Phys., 18, 5515-5528, 10.5194/acp-18-5515-2018, 2018.
Holland, F., Hofzumahaus, A., Schafer, R., Kraus, A., and Patz, H. W.: Measurements of OH and HO2 radical concentrations and photolysis frequencies during BERLIOZ, J. Geophys. Res.-Atmos., 108, 22, 10.1029/2001jd001393, 2003.
Hou, S., Tong, S., Ge, M., and An, J.: Comparison of atmospheric nitrous acid during severe haze and clean periods in Beijing, China, Atmos. Environ., 124, 199-206, https://doi.org/10.1016/j.atmosenv.2015.06.023, 2016.
Huang, L., Zhao, Y., Li, H., and Chen, Z.: Kinetics of Heterogeneous Reaction of Sulfur Dioxide on Authentic Mineral Dust: Effects of Relative Humidity and Hydrogen Peroxide, Environ. Sci. Technol., 49, 10797-10805, 10.1021/acs.est.5b03930, 2015.
Huang, R.-J., Zhang, Y., Bozzetti, C., Ho, K.-F., Cao, J.-J., Han, Y., Daellenbach, K. R., Slowik, J. G., Platt, S. M., Canonaco, F., Zotter, P., Wolf, R., Pieber, S. M., Bruns, E. A., Crippa, M., Ciarelli, G., Piazzalunga, A., Schwikowski, M., Abbaszade, G., Schnelle-Kreis, J., Zimmermann, R., An, Z., Szidat, S., Baltensperger, U., Haddad, I. E., and Prevot, A. S. H.: High secondary aerosol contribution to particulate pollution during haze events in China, Nature, 514(7521), 218-222, 10.1038/nature13774, 2014.
Huang, R.-J., Yang, L., Cao, J., Wang, Q., Tie, X., Ho, K.-F., Shen, Z., Zhang, R., Li, G., Zhu, C., Zhang, N., Dai, W., Zhou, J., Liu, S., Chen, Y., Chen, J., and O'Dowd, C. D.: Concentration and sources of

https://doi.org/10.5194/acp-2020-150
Preprint. Discussion started: 21 February 2020


Atmospheric Chemistry and Physics Discussions

atmospheric nitrous acid (HONO) at an urban site in Western China, Sci. Total Environ., 593, 165-172, 10.1016/j.scitotenv.2017.02.166, 2017.

Kanaya, Y., Cao, R., Akimoto, H., Fukuda, M., Komazaki, Y., Yokouchi, Y., Koike, M., Tanimoto, H., Takegawa, N., and Kondo, a. Y.: Urban photochemistry in central Tokyo: 1. Observed and modeled OH and HO2 radical concentrations during the winter and summer of 2004, J. Geophy. Res.- Atmos., 112, 10.1029/2007JD008670, 2007.

Kim, S., VandenBoer, T. C., Young, C. J., Riedel, T. P., Thornton, J. A., Swarthout, B., Sive, B., Lerner, B., Gilman, J. B., Warneke, C., Roberts, J. M., Guenther, A., Wagner, N. L., Dubé, W. P., Williams, E., and Brown, S. S.: The primary and recycling sources of OH during the NACHTT-2011 campaign: HONO as an important OH primary source in the wintertime, J. Geophys. Res.- Atmos., 119, 6886-6896, doi:10.1002/2013JD019784, 2014.

Kroll, J. H., and Seinfeld, J. H.: Chemistry of secondary organic aerosol: Formation and evolution of low-volatility organics in the atmosphere, Atmos. Environ., 42, 3593-3624, 2008.

Kulmala, M.: Build a global Earth observatory, Nature, 553, 21-23, 10.1038/d41586-017-08967-y, 2018.

Lang, J., Zhang, Y., Zhou, Y., Cheng, S., Chen, D., Guo, X., Chen, S., Li, X., Xing, X., and Wang, H.: Trends of PM2.5 and Chemical Composition in Beijing, 2000-2015, Aerosol Air Qual. Res., 17, 412-425, 10.4209/aaqr.2016.07.0307, 2017.

Lee, J. D., Whalley, L. K., Heard, D. E., Stone, D., Dunmore, R. E., Hamilton, J. F., Young, D. E., Allan, J. D., Laufs, S., and Kleffmann, J.: Detailed budget analysis of HONO in central London reveals a missing daytime source, Atmos. Chem. Phys., 16, 2747-2764, 10.5194/acp-16-2747-2016, 2016.

Lelieveld, J., Evans, J. S., Fnais, M., Giannadaki, D., and Pozzer, A.: The contribution of outdoor air pollution sources to premature mortality on a global scale, Nature, 525, 367-371, 10.1038/nature15371, 2015.

Li, D., Xue, L., Wen, L., Wang, X., Chen, T., Mellouki, A., Chen, J., and Wang, W.: Characteristics and sources of nitrous acid in an urban atmosphere of northern China: Results from 1-yr continuous observations, Atmos. Environ., 182, 296-306, https://doi.org/10.1016/j.atmosenv.2018.03.033, 2018.

Li, X., Brauers, T., H ̈aseler, R., Bohn, B., Fuchs, H., Hofzumahaus, A., Holland, F., Lou, S., Lu, K. D., Rohrer, F., Hu, M., Zeng, L. M., Zhang, Y. H., Garland, R. M., Su, H., Nowak, A., Wiedensohler, A., Takegawa, N., Shao, M., and Wahner, A.: Exploring the atmospheric chemistry of nitrous acid (HONO) at a rural site in Southern China, Atmos. Chem. Phys., 12, 1497-1513, 2012.

Li, Z. Q., Guo, J. P., Ding, A. J., Liao, H., Liu, J. J., Sun, Y. L., Wang, T. J., Xue, H. W., Zhang, H. S., and Zhu, B.: Aerosol and boundary-layer interactions and impact on air quality, Natl. Sci. Rev., 4, 810-833, 10.1093/nsr/nwx117, 2017.

Liu, C., Ma, Z., Mu, Y., Liu, J., Zhang, C., Zhang, Y., Liu, P., and Zhang, H.: The levels, variation characteristics, and sources of atmospheric non-methane hydrocarbon compounds during wintertime in Beijing, China, Atmos. Chem. Phys., 17, 10633-10649, 10.5194/acp-17-10633-2017, 2017a.

Liu, F., Beirle, S., Zhang, Q., van der A, R. J., Zheng, B., Tong, D., and He, K.: NOx emission trends over Chinese cities estimated from OMI observations during 2005 to 2015, Atmos. Chem. Phys., 17, 9261-9275, 10.5194/acp-17-9261-2017, 2017b.

Liu, J., Li, S., Mekic, M., Jiang, H., Zhou, W., Loisel, G., Song, W., Wang, X., and Gligorovski, S.: Photoenhanced Uptake of NO2 and HONO Formation on Real Urban Grime, Environ. Sci. Technol. Lett., 6, 413-417, 10.1021/acs.estlett.9b00308, 2019a.

Liu, T., Gong, S., He, J., Yu, M., Wang, Q., Li, H., Liu, W., Zhang, J., Li, L., Wang, X., Li, S., Lu, Y., Du, H., Wang, Y., Zhou, C., Liu, H., and Zhao, Q.: Attributions of meteorological and emission factors to the

https://doi.org/10.5194/acp-2020-150
Preprint. Discussion started: 21 February 2020


Atmospheric Chemistry and Physics Discussions

745 2015 winter severe haze pollution episodes in China's Jing-Jin-Ji area, Atmos. Chem. Phys., 17, 2971-
746 2980, 10.5194/acp-17-2971-2017, 2017c.
747 Liu, Y., Han, C., Ma, J., Bao, X., and He, H.: Influence of relative humidity on heterogeneous kinetics of
748 NO2 on kaolin and hematite, Phys. Chem. Chem. Phys., 17, 19424-19431, doi: 10.1039/C5CP02223A,
749 2015.
750 Liu, Y., Lu, K., Ma, Y., Yang, X., Zhang, W., Wu, Y., Peng, J., Shuai, S., Hu, M., and Zhang, Y.: Direct
751 emission of nitrous acid (HONO) from gasoline cars in China determined by vehicle chassis
752 dynamometer experiments, Atmos. Environ., 169, 89-96, 10.1016/j.atmosenv.2017.07.019, 2017d.
753 Liu, Y., Nie, W., Xu, Z., Wang, T., Wang, R., Li, Y., Wang, L., Chi, X., and Ding, A.: Contributions of
754 different sources to nitrous acid (HONO) at the SORPES station in eastern China: results from one-year
755 continuous observation, Atmos. Chem. Phys. Discuss., 2019, 1-47, 10.5194/acp-2019-219, 2019b.
756 Liu, Y. H., Lu, K. D., Li, X., Dong, H. B., Tan, Z. F., Wang, H. C., Zou, Q., Wu, Y. S., Zeng, L. M., Hu,
757 M., Min, K. E., Kecorius, S., Wiedensohler, A., and Zhang, Y. H.: A Comprehensive Model Test of the
758 HONO Sources Constrained to Field Measurements at Rural North China Plain, Environ. Sci. Technol.,
759 53, 3517-3525, 10.1021/acs.est.8b06367, 2019c.
760 Meusel, H., Tamm, A., Kuhn, U., Wu, D., Leifke, A. L., Fiedler, S., Ruckteschler, N., Yordanova, P.,
761 Lang-Yona, N., Poehlker, M., Lelieveld, J., Hoffmann, T., Poeschl, U., Su, H., Weber, B., and Cheng, Y.:
762 Emission of nitrous acid from soil and biological soil crusts represents an important source of HONO in
763 the remote atmosphere in Cyprus, Atmos. Chem. Phys., 18, 799-813, 10.5194/acp-18-799-2018, 2018.
764 Michoud, V., Colomb, A., Borbon, A., Miet, K., Beekmann, M., Camredon, M., Aumont, B., Perrier, S.,
765 Zapf, P., Siour, G., Ait-Helal, W., Afif, C., Kukui, A., Furger, M., Dupont, J. C., Haeffelin, M., and
766 Doussin, J. F.: Study of the unknown HONO daytime source at a European suburban site during the
767 MEGAPOLI summer and winter field campaigns, Atmos. Chem. Phys., 14, 2805-2822, 10.5194/acp-14-
768 2805-2014, 2014.
769 Ndour, M., D'Anna, B., George, C., Ka, O., Balkanski, Y., K., J., S., and K., A., M.,: Photoenhanced
770 uptake of NO2 on mineral dust: Laboratory experiments and model simulations, Geophys. Res. Lett., 35,
771 L05812. doi:05810.01029/02007GL032006, 2008.
772 Ndour, M., Nicolas, M., D'Anna, B., Ka, O., and George, C.: Photoreactivity of NO2 on mineral dusts
773 originating from different locations of the Sahara desert, Phys. Chem. Chem. Phys., 11, 1312-1319, 2009.
774 Oswald, R., Behrendt, T., Ermel, M., Wu, D., Su, H., Cheng, Y., Breuninger, C., Moravek, A., Mougin,
775 E., Delon, C., Loubet, B., Pommerening-Röser, A., Sörgel, M., Pöschl, U., Hoffmann, T., Andreae, M.
776 O., Meixner, F. X., and Trebs, I.: HONO Emissions from Soil Bacteria as a Major Source of Atmospheric
777 Reactive Nitrogen, Science, 341, 1233-1235, 10.1126/science.1242266, 2013.
778 Oswald, R., Ermel, M., Hens, K., Novelli, A., Ouwersloot, H. G., Paasonen, P., Petäjä, T., Sipilä, M.,
779 Keronen, P., Bäck, J., Königstedt, R., Hosaynali Beygi, Z., Fischer, H., Bohn, B., Kubistin, D., Harder,
780 H., Martinez, M., Williams, J., Hoffmann, T., Trebs, I., and Sörgel, M.: A comparison of HONO budgets
781 for two measurement heights at a field station within the boreal forest in Finland, Atmos. Chem. Phys.,
782 15, 799-813, 10.5194/acp-15-799-2015, 2015.
783 Qin, M., Xie, P., Su, H., Gu, J., Peng, F., Li, S., Zeng, L., Liu, J., Liu, W., and Zhang, Y.: An observational
784 study of the HONO-NO2 coupling at an urban site in Guangzhou City, South China, Atmos. Environ.,
785 43, 5731-5742, 10.1016/j.atmosenv.2009.08.017, 2009.
786 Ren, X., Brune, W. H., Mao, J., Mitchell, M. J., Lesher, R. L., Simpas, J. B., Metcalf, A. R., Schwab, J.
787 J., Cai, C., Li, Y., Demerjian, K. L., Felton, H. D., Boynton, G., Adams, A., Perry, J., He, Y., Zhou, X.,
788 and Hou, J.: Behavior of OH and HO2 in the winter atmosphere in New York City, Atmos. Environ., 40,

https://doi.org/10.5194/acp-2020-150
Preprint. Discussion started: 21 February 2020




252-263, https://doi.org/10.1016/j.atmosenv.2005.11.073, 2006.

Rohrer, F., Bohn, B., Brauers, T., Bruning, D., Johnen, F. J., Wahner, A., and Kleffmann, J.: Characterisation of the photolytic HONO-source in the atmosphere simulation chamber SAPHIR, Atmos. Chem. Phys., 5, 2189-2201, 10.5194/acp-5-2189-2005, 2005.

Sangwan, M., and Zhu, L.: Role of Methyl-2-nitrophenol Photolysis as a Potential Source of OH Radicals in the Polluted Atmosphere: Implications from Laboratory Investigation, J. Phys. Chem. A, 122, 1861-1872, 10.1021/acs.jpca.7b11235, 2018.

Seinfeld, J. H., and Pandis, S. N.: Atmospheric chemistry and physics: From air pollution to climate change, Second ed., John Wiley and Sons, New Jersey, 2006.

Spataro, F., Ianniello, A., Esposito, G., Allegrini, I., Zhu, T., and Hu, M.: Occurrence of atmospheric nitrous acid in the urban area of Beijing (China), Sci. Total Environ., 447, 210-224, https://doi.org/10.1016/j.scitotenv.2012.12.065, 2013.

Stutz, J., Wong, K. W., and Tsai, C.: Field Observations of Daytime HONO Chemistry and Its Impact on the OH Radical Budget, in: Disposal of Dangerous Chemicals in Urban Areas and Mega Cities, Dordrecht, 2013, 1-14.

Su, P. H., Kuo, D. T. F., Shih, Y. H., and Chen, C. Y.: Sorption of organic compounds to two diesel soot black carbons in water evaluated by liquid chromatography and polyparameter linear solvation energy relationship, Water Res., 144, 709-718, 10.1016/j.watres.2018.07.064, 2018.

Sun, Y. L., Wang, Z. F., Fu, P. Q., Yang, T., Jiang, Q., Dong, H. B., Li, J., and Jia, J. J.: Aerosol composition, sources and processes during wintertime in Beijing, China, Atmos. Chem. Phys., 13, 4577-4592, 10.5194/acp-13-4577-2013, 2013.

Sun, Y. L., Wang, Z. F., Du, W., Zhang, Q., Wang, Q. Q., Fu, P. Q., Pan, X. L., Li, J., Jayne, J., and Worsnop, D. R.: Long-term real-time measurements of aerosol particle composition in Beijing, China: seasonal variations, meteorological effects, and source analysis, Atmos. Chem. Phys., 15, 10149-10165, 10.5194/acp-15-10149-2015, 2015.

Tan, Z., Fuchs, H., Lu, K., Hofzumahaus, A., Bohn, B., Broch, S., Dong, H., Gomm, S., Häseler, R., He, L., Holland, F., Li, X., Liu, Y., Lu, S., Rohrer, F., Shao, M., Wang, B., Wang, M., Wu, Y., Zeng, L., Zhang, Y., Wahner, A., and Zhang, Y.: Radical chemistry at a rural site (Wangdu) in the North China Plain: observation and model calculations of OH, HO2 and RO2 radicals, Atmos. Chem. Phys., 17, 663-690, 10.5194/acp-17-663-2017, 2017.

Tan, Z., Rohrer, F., Lu, K., Ma, X., Bohn, B., Broch, S., Dong, H., Fuchs, H., Gkatzelis, G. I., Hofzumahaus, A., Holland, F., Li, X., Liu, Y., Liu, Y., Novelli, A., Shao, M., Wang, H., Wu, Y., Zeng, L., Hu, M., Kiendler-Scharr, A., Wahner, A., and Zhang, Y.: Wintertime photochemistry in Beijing: observations of ROx radical concentrations in the North China Plain during the BEST-ONE campaign, Atmos. Chem. Phys., 18, 12391-12411, 10.5194/acp-18-12391-2018, 2018.

Tan, Z. F., Lu, K. D., Jiang, M. Q., Su, R., Wang, H. L., Lou, S. R., Fu, Q. Y., Zhai, C. Z., Tan, Q. W., Yue, D. L., Chen, D. H., Wang, Z. S., Xie, S. D., Zeng, L. M., and Zhang, Y. H.: Daytime atmospheric oxidation capacity in four Chinese megacities during the photochemically polluted season: a case study based on box model simulation, Atmos. Chem. Phys., 19, 3493-3513, 10.5194/acp-19-3493-2019, 2019.

Tang, Y., An, J., Wang, F., Li, Y., Qu, Y., Chen, Y., and Lin, J.: Impacts of an unknown daytime HONO source on the mixing ratio and budget of HONO, and hydroxyl, hydroperoxyl, and organic peroxy radicals, in the coastal regions of China, Atmos. Chem. Phys., 15, 9381-9398, 10.5194/acp-15-9381-2015, 2015.

Tian, M., Liu, Y., Yang, F. M., Zhang, L. M., Peng, C., Chen, Y., Shi, G. M., Wang, H. B., Luo, B., Jiang,

https://doi.org/10.5194/acp-2020-150
Preprint. Discussion started: 21 February 2020


Atmospheric Chemistry and Physics Discussions

C. T., Li, B., Takeda, N., and Koizumi, K.: Increasing importance of nitrate formation for heavy aerosol pollution in two megacities in Sichuan Basin, southwest China, Environ. Pollut., 250, 898-905, 10.1016/j.envpol.2019.04.098, 2019.

Tong, S., Hou, S., Zhang, Y., Chu, B., Liu, Y., He, H., Zhao, P., and Ge, M.: Exploring the nitrous acid (HONO) formation mechanism in winter Beijing: direct emissions and heterogeneous production in urban and suburban areas, Faraday Discuss., 189, 213-230, 10.1039/c5fd00163c, 2016.

Trinh, H. T., Imanishi, K., Morikawa, T., Hagino, H., and Takenaka, N.: Gaseous nitrous acid (HONO) and nitrogen oxides (NOx) emission from gasoline and diesel vehicles under real-world driving test cycles, J. Air Waste Manage. Assoc., 67, 412-420, 10.1080/10962247.2016.1240726, 2017.

Underwood, G. M., Miller, T. M., and Grassian, V. H.: Transmission FT-IR and Knudsen Cell Study of the Heterogeneous Reactivity of Gaseous Nitrogen Dioxide on Mineral Oxide Particles, J. Phys. Chem. A, 103 6184-6190, 1999.

Underwood, G. M., Song, C. H., Phadnis, M., Carmichael, G. R., and Grassian, V. H.: Heterogeneous reactions of NO2 and HNO3 on oxides and mineral dust: A combined laboratory and modeling study, J. Geophy. Res.- Atmos., 106, 18055-18066, 10.1029/2000jd900552, 2001.

Volkamer, R., Sheehy, P., Molina, L. T., and Molina, M. J.: Oxidative capacity of the Mexico City atmosphere – Part 1: A radical source perspective, Atmos. Chem. Phys., 10, 6969-6991, 10.5194/acp-10-6969-2010, 2010.

Vu, T. V., Shi, Z., Cheng, J., Zhang, Q., He, K., Wang, S., and Harrison, R. M.: Assessing the impact of Clean Air Action Plan on Air Quality Trends in Beijing Megacity using a machine learning technique, Atmos. Chem. Phys. Discuss., 2019, 1-18, 10.5194/acp-2019-173, 2019.

Wang, G., Zhang, R., Gomez, M. E., Yang, L., Zamora, M. L., Hu, M., Lin, Y., Peng, J., Guoc, S., Meng, J., Li, J., Cheng, C., Hu, T., Ren, Y., Wang, Y., Gao, J., Cao, J., An, Z., Zhou, W., Li, G., Wang, J., Tian, P., Marrero-Ortiz, W., Secrest, J., Du, Z., Zheng, J., Shang, D., Zeng, L., Shao, M., Wang, W., Huang, Y., Wang, Y., Zhu, Y., Li, Y., Hu, J., Pan, B., Cai, L., Cheng, Y., Ji, Y., Zhang, F., Rosenfeld, D., Liss, P. S., Duce, R. A., Kolb, C. E., and Molina, M. J.: Persistent sulfate formation from London Fog to Chinese haze, Proc. Natl. Acad. Sci. USA, 113, 13630-13635, 2016.

Wang, H., Lu, K., Chen, X., Zhu, Q., Chen, Q., Guo, S., Jiang, M., Li, X., Shang, D., Tan, Z., Wu, Y., Wu, Z., Zou, Q., Zheng, Y., Zeng, L., Zhu, T., Hu, M., and Zhang, Y.: High $N_2O_5$ Concentrations Observed in Urban Beijing: Implications of a Large Nitrate Formation Pathway, Environ. Sci. Technol. Lett., 4, 416-420, 10.1021/acs.estlett.7b00341, 2017a.

Wang, H. C., Lu, K. D., Chen, X. R., Zhu, Q. D., Wu, Z. J., Wu, Y. S., and Sun, K.: Fast particulate nitrate formation via N2O5 uptake aloft in winter in Beijing, Atmos. Chem. Phys., 18, 10483-10495, 10.5194/acp-18-10483-2018, 2018.

Wang, J., Zhang, X., Guo, J., Wang, Z., and Zhang, M.: Observation of nitrous acid (HONO) in Beijing, China: Seasonal variation, nocturnal formation and daytime budget, Sci. Total Environ., 587, 350-359, 10.1016/j.scitotenv.2017.02.159, 2017b.

Wang, S., Nan, J., Shi, C., Fu, Q., Gao, S., Wang, D., Cui, H., Saiz-Lopez, A., and Zhou, B.: Atmospheric ammonia and its impacts on regional air quality over the megacity of Shanghai, China, Sci. Rep., 5, 15842-15842, 10.1038/srep15842, 2015.

Wang, Y. L., Song, W., Yang, W., Sun, X. C., Tong, Y. D., Wang, X. M., Liu, C. Q., Bai, Z. P., and Liu, X. Y.: Influences of Atmospheric Pollution on the Contributions of Major Oxidation Pathways to PM2.5 Nitrate Formation in Beijing, J. Geophys. Res.-Atmos., 124, 4174-4185, 10.1029/2019jd030284, 2019.

Wang, Y. S., Teter, J., and Sperling, D.: China's soaring vehicle population: Even greater than forecasted?,

https://doi.org/10.5194/acp-2020-150
Preprint. Discussion started: 21 February 2020




Energy Policy, 39, 3296-3306, 10.1016/j.enpol.2011.03.020, 2011.

Wang, Z., Wang, W., Tham, Y. J., Li, Q., Wang, H., Wen, L., Wang, X., and Wang, T.: Fast heterogeneous N2O5 uptake and ClNO2 production in power plant and industrial plumes observed in the nocturnal residual layer over the North China Plain, Atmos. Chem. Phys., 17, 12361-12378, 10.5194/acp-17-12361-2017, 2017c.

Xing, L., Wu, J., Elser, M., Tong, S., Liu, S., Li, X., Liu, L., Cao, J., Zhou, J., El-Haddad, I., Huang, R., Ge, M., Tie, X., Prévôt, A. S. H., and Li, G.: Wintertime secondary organic aerosol formation in Beijing–Tianjin–Hebei (BTH): contributions of HONO sources and heterogeneous reactions, Atmos. Chem. Phys., 19, 2343-2359, 10.5194/acp-19-2343-2019, 2019.

Xu, Z., Wang, T., Wu, J., Xue, L., Chan, J., Zha, Q., Zhou, S., Louie, P. K. K., and Luk, C. W. Y.: Nitrous acid (HONO) in a polluted subtropical atmosphere: Seasonal variability, direct vehicle emissions and heterogeneous production at ground surface, Atmos. Environ., 106, 100-109, 10.1016/j.atmosenv.2015.01.061, 2015.

Yang, D., Zhang, S., Niu, T., Wang, Y., Xu, H., Zhang, K. M., and Wu, Y.: High-resolution mapping of vehicle emissions of atmospheric pollutants based on large-scale, real-world traffic datasets, Atmos. Chem. Phys. Discuss., 2019, 1-22, 10.5194/acp-2019-32, 2019.

Yang, Q., Su, H., Li, X., Cheng, Y., Lu, K., Cheng, P., Gu, J., Guo, S., Hu, M., Zeng, L., Zhu, T., and Zhang, Y.: Daytime HONO formation in the suburban area of the megacity Beijing, China, Science China-Chemistry, 57, 1032-1042, 10.1007/s11426-013-5044-0, 2014.

Zhang, F., Wang, Y., Peng, J., Chen, L., Sun, Y., Duan, L., Ge, X., Li, Y., Zhao, J., Liu, C., Zhang, X., Zhang, G., Pan, Y., Wang, Y., Zhang, A. L., Ji, Y., Wang, G., Hu, M., Molina, M. J., and Zhang, R.: An unexpected catalyst dominates formation and radiative forcing of regional haze, Proc. Natl. Acad. Sci. USA, 201919343, 10.1073/pnas.1919343117, 2020.

Zhang, J., An, J., Qu, Y., Liu, X., and Chen, Y.: Impacts of potential HONO sources on the concentrations of oxidants and secondary organic aerosols in the Beijing-Tianjin-Hebei region of China, Sci. Total Environ., 647, 836-852, https://doi.org/10.1016/j.scitotenv.2018.08.030, 2019a.

Zhang, J. M., Yang, L. X., Chen, J. M., Mellouki, A., Jiang, P., Gao, Y., Li, Y. Y., Yang, Y. M., and Wang, W. X.: Influence of fireworks displays on the chemical characteristics of PM2.5 in rural and suburban areas in Central and East China, Sci. Total Environ., 578, 476-484, 10.1016/j.scitotenv.2016.10.212, 2017.

Zhang, J. W., Chen, J. M., Xue, C. Y., Chen, H., Zhang, Q., Liu, X. G., Mu, Y. J., Guo, Y. T., Wang, D. Y., Chen, Y., Li, J. L., Qu, Y., and An, J. L.: Impacts of six potential HONO sources on HOx budgets and SOA formation during a wintertime heavy haze period in the North China Plain, Sci. Total Environ., 681, 110-123, 10.1016/j.scitotenv.2019.05.100, 2019b.

Zhang, X. Y., Zhong, J. T., Wang, J. Z., Wang, Y. Q., and Liu, Y. J.: The interdecadal worsening of weather conditions affecting aerosol pollution in the Beijing area in relation to climate warming, Atmos. Chem. Phys., 18, 5991-5999, 10.5194/acp-18-5991-2018, 2018.

Zheng, B., Zhang, Q., Zhang, Y., He, K. B., Wang, K., Zheng, G. J., Duan, F. K., Ma, Y. L., and Kimoto, T.: Heterogeneous chemistry: a mechanism missing in current models to explain secondary inorganic aerosol formation during the January 2013 haze episode in North China, Atmos. Chem. Phys., 15, 2031-2049, doi: 10.5194/acp-15-2031-2015, 2015a.

Zheng, G. J., Duan, F. K., Su, H., Ma, Y. L., Cheng, Y., Zheng, B., Zhang, Q., Huang, T., Kimoto, T., Chang, D., Pöschl, U., Cheng, Y. F., and He, K. B.: Exploring the severe winter haze in Beijing: the impact of synoptic weather, regional transport and heterogeneous reactions, Atmos. Chem. Phys., 15,

https://doi.org/10.5194/acp-2020-150
Preprint. Discussion started: 21 February 2020


Atmospheric Chemistry and Physics Discussions

921 2969-2983, 10.5194/acp-15-2969-2015, 2015b.
922 Zhu, W. H., Xu, X. D., Zheng, J., Yan, P., Wang, Y. J., and Cai, W. Y.: The characteristics of abnormal
923 wintertime pollution events in the Jing-Jin-Ji region and its relationships with meteorological factors, Sci.
924 Total Environ., 626, 887-898, 10.1016/j.scitotenv.2018.01.083, 2018.
925
926

https://doi.org/10.5194/acp-2020-150
Preprint. Discussion started: 21 February 2020


Atmospheric Chemistry and Physics Discussions

## Figure captions

Fig. 1. An overviewed measurement of non-refractory-$PM_{2.5}$ (NR-$PM_{2.5}$) and HONO from Feb. 1 to July 1, 2018. (A) the mass concentration of different components of $PM_{2.5}$ and (B) the mass fraction of individual component and (C) HONO concentration and UVB intensity during observation. We consider the period before Apr. 1 as winter. During the winter period, 12 cases are selected and numbered, including three clean cases (1, 3, and 5, marked in yellow) and the rest 9 pollution episodes (marked in blue).

**Fig. 2.** Contribution of HONO to OH production and correlation between OA and HONO concentration. Diurnal production rates of OH from photolysis of HONO and $O_3$ in polluted days with $PM_{2.5}$ concentration larger than 50 μg $m^{-3}$ and RH less than 90 % (A) from Feb 1 to Mar 31, (B) from Apr 1 to Jun 30; (C) Daytime variation of OA/CO and HONO/CO concentration for the $7^{th}$ and $12^{th}$ episodes and (D) correlation of the daytime OA/CO increased and consumed HONO/CO.

**Fig. 3.** Diurnal pattern of HONO sources calculated with different parameterizations. The low bound, the middle value, and upper bound of (A) soil emission calculated based on 45-55%, 35-45% and 25-35% of water content, (B) vehicle emission with relative emission factor to NOx of 0.18%, 1.17±0.05% and 1.8 %, (C) production from reaction between NO and OH, whose concentration estimated using Xu (Xu et al., 2015), (Tan et al., 2019)

**Fig. 4.** The budget of HONO (A) and (B) Diurnal production rates of HONO, (C) and (D) loss rates of HONO, (E) and (F) relative contribution of each source in polluted days with $PM_{2.5}$ concentrations higher than 50 μg $m^{-3}$ and RH less than 90 %. The left

https://doi.org/10.5194/acp-2020-150
Preprint. Discussion started: 21 February 2020


Atmospheric Chemistry and Physics Discussions

column shows the data from February 1 to March 31) and the right one shows the data from April 1 to June 30.

**Fig. 5.** (A)-(B) Diurnal production rates and (C)-(D) diurnal loss rates of HONO; (E)-(F) relative contribution of HONO sources in polluted days with $PM_{2.5}$ concentrations higher than 50 μg $m^{-3}$ and RH less than 90 %. The $E_{vehicle}$ is calculated using the low limit of HONO/NOx from vehicles (0.18%) (Liu et al., 2017d) and the $P_{NO\text{-}OH}$ is calculated using the low limit of OH concentration, while the upper limit of $E_{soil}$, $P_{aerosol}$ and $P_{ground}$ are used as described in the text.

https://doi.org/10.5194/acp-2020-150
Preprint. Discussion started: 21 February 2020


Atmospheric Chemistry and Physics Discussions

957 **Figures**

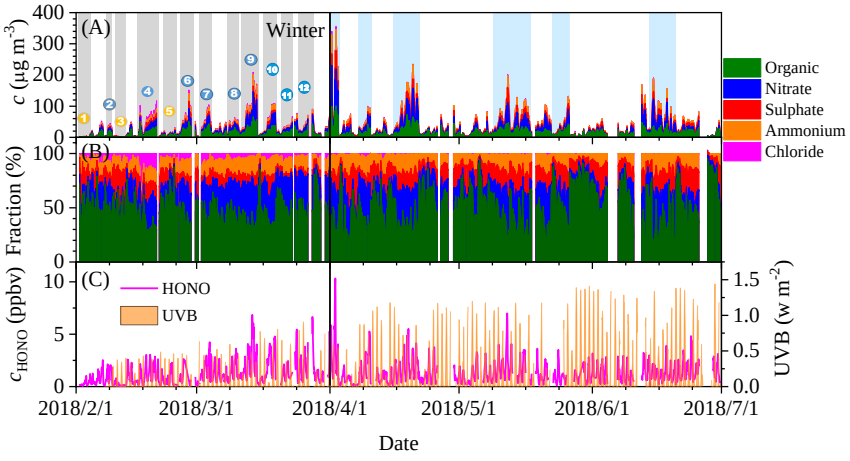


958

959 **Fig. 1**.

960

https://doi.org/10.5194/acp-2020-150
Preprint. Discussion started: 21 February 2020


Atmospheric Chemistry and Physics Discussions

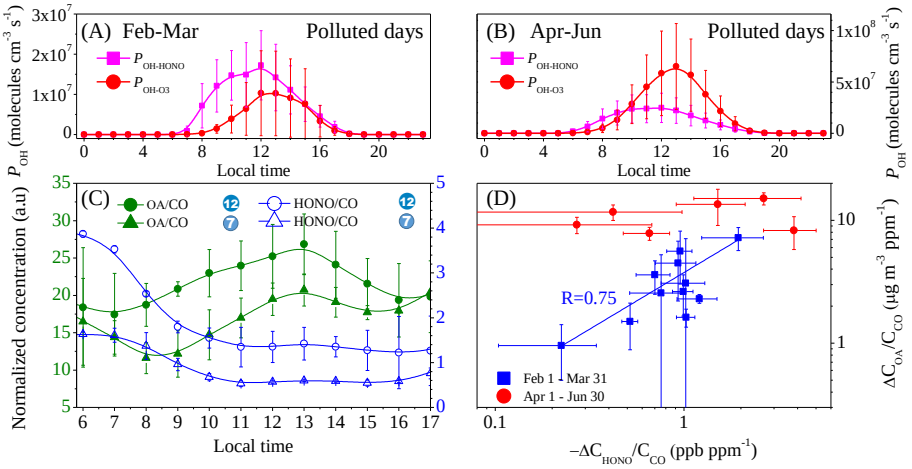


961

962 **Fig. 2.**

963

https://doi.org/10.5194/acp-2020-150
Preprint. Discussion started: 21 February 2020


Atmospheric Chemistry and Physics Discussions

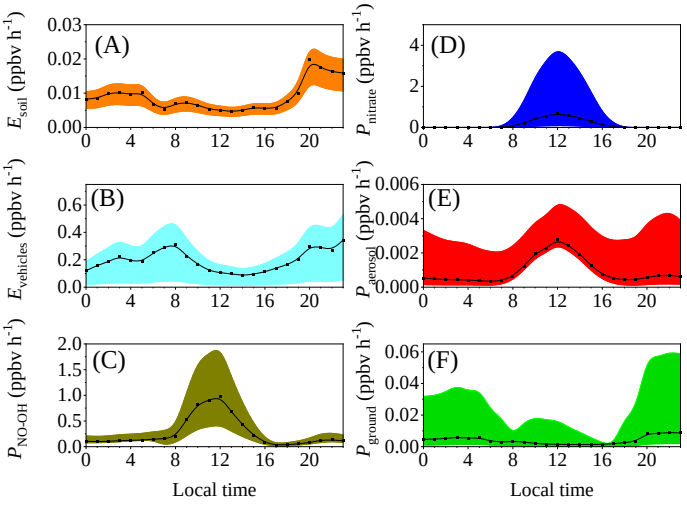


964

965 **Fig. 3**

966

https://doi.org/10.5194/acp-2020-150
Preprint. Discussion started: 21 February 2020


Atmospheric Chemistry and Physics Discussions

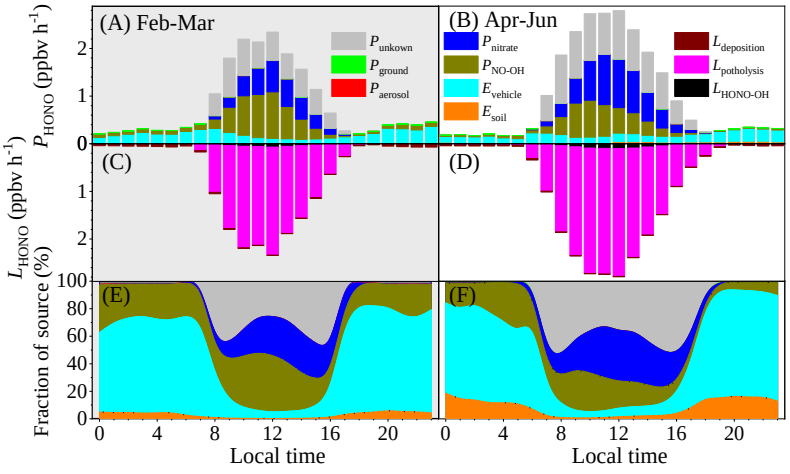


967

968 **Fig. 4.**

969

https://doi.org/10.5194/acp-2020-150
Preprint. Discussion started: 21 February 2020


Atmospheric Chemistry and Physics Discussions

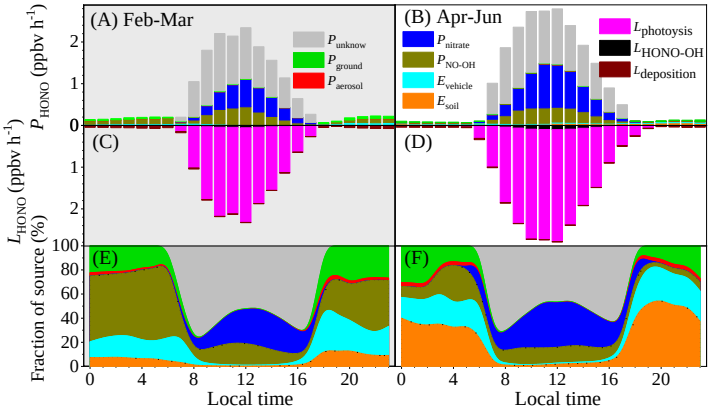


970

971 **Fig. 5.**